# *Dynamic methylation pattern of* cyp19a1a *core promoter during zebrafish ovarian folliculogenesis*

**Jin Bai, Weida Gong, Cuili Wang, Yida Gao, Wanshu Hong & Shi Xi Chen**

**Fish Physiology and Biochemistry**

ISSN 0920-1742

Fish Physiol Biochem
DOI 10.1007/s10695-015-0187-x

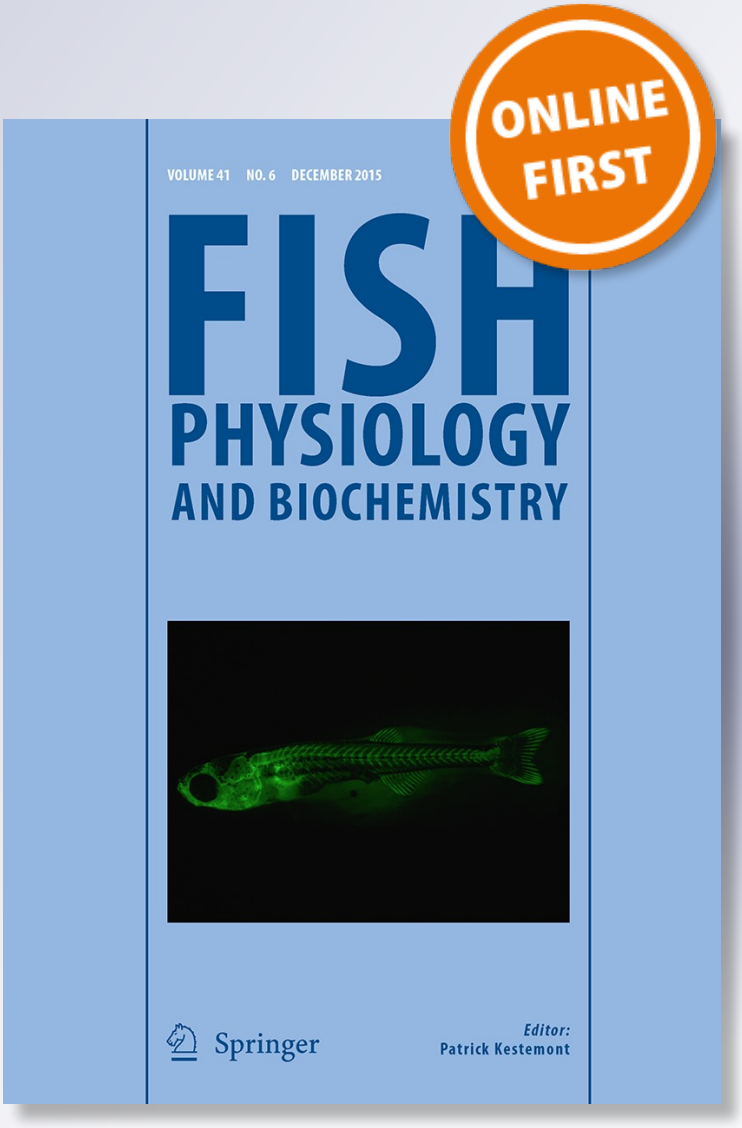


Springer

Fish Physiol Biochem
DOI 10.1007/s10695-015-0187-x

# Dynamic methylation pattern of *cyp19a1a* core promoter during zebrafish ovarian folliculogenesis

**Jin Bai · Weida Gong · Cuili Wang · Yida Gao · Wanshu Hong · Shi Xi Chen**

Received: 22 July 2015 / Accepted: 21 December 2015


**Abstract** In vertebrates, the aromatase coded by the *cyp19a1a* gene can catalyze the conversion from androgens to estrogens. Thus, the regulatory mechanisms of *cyp19a1a* gene expression are a critical research field in reproductive endocrinology. In this study, we use zebrafish as a model to study the dynamic methylation levels of the *cyp19a1a* gene core promoter during zebrafish ovarian folliculogenesis. The results show that there is an apparent fluctuation of the methylation levels of zebrafish *cyp19a1a* core promoter. Moreover, the methylation levels are inversely correlated with the expression levels of *cyp19a1a* transcripts when the ovarian follicles develop from PV into the MV stage. Also, the CpG dinucleotides which are close to the transcriptional starting site may have provided a significant blocking effect on inhibiting the transcriptional function of RNA polymerase II. Taken together, the results from the present study strongly suggest that DNA methylation was one of mechanisms that are involved in the regulation of *cyp19a1a* gene expression during folliculogenesis. This methylation mechanism modifying transcriptional process accompanied with zebrafish ovarian folliculogenesis might also shed new light on the regulation of *cyp19a1a* expression during the ovarian developmental stage in other vertebrates.

**Keywords** *cyp19a1a* gene · DNA methylation · Ovarian folliculogenesis · Zebrafish (*Danio rerio*)

C. Wang · W. Hong · S. X. Chen (✉)
State Key Laboratory of Marine Environmental Science, Xiamen University, Xiamen 361102, China
e-mail: chenshixi@xmu.edu.cn

J. Bai · W. Gong · C. Wang · Y. Gao · W. Hong · S. X. Chen
College of Ocean and Earth Sciences, Xiamen University, Xiamen 361102, China

W. Hong · S. X. Chen
Fujian Engineering Laboratory of Marine Bioproducts and Technology, Xiamen University, Xiamen 361102, China

W. Hong · S. X. Chen
Fujian Collaborative Innovation Center for Exploitation and Utilization of Marine Biological Resources, Xiamen 361102, China

## Introduction

Members of the cytochrome P450 superfamily exert a pivotal function in catalyzing the oxidation of organic substances (Guengerich 2007). As a member of the cytochrome P450 superfamily, aromatase is an enzyme complex that catalyzes the biosynthesis of estrogens from the androgens (Duffy et al. 2010). In the vast majority of tetrapods examined so far, aromatase is the product of the *cyp19* gene, which exists as a single copy per haploid genome (Piferrer and Blázquez 2005). In contrast, in teleosts there are two isoforms of the aromatase gene, *cyp19a1a* and *cyp19a1b*, which encode two structurally different

Published online: 30 December 2015

proteins, i.e., P450aromA and P450aromB, with similar catalytic activities. The *cyp19a1a* is specifically expressed in the gonad, while the *cyp19a1b* is specifically expressed in the brain (Tchoudakova and Callard 1998). Because estrogen plays several important roles in reproductive endocrinology, the regulatory mechanisms of *cyp19a1a* gene expression have received greater attention (Piferrer and Blázquez 2005).

Recent studies suggest that epigenetic mechanisms may regulate *cyp19a* expression in mammals including humans (Knower et al. 2010), sheep (Fürbass et al. 2008), buffalo (Monga et al. 2011), and rat (Lee et al. 2012). In fish, a study in European sea bass (*Dicentrarchus labrax*) indicates that DNA methylation of the *cyp19a* promoter may be an essential component of the mechanism connecting environmental temperature and sex ratios (Navarro-Martín et al. 2011). Another study in ricefield eel (*Monopterus albus*), a protogynous hermaphrodite fish, suggests that the epigenetic mechanisms involved in DNA methylation of *cyp19a1a* promoter may be a mechanism to drive the sex change (Zhang et al. 2013). In addition to its critical role during sex determination, 17β-estradiol ($E_2$) produced in the granulosa cells of the follicular layers surrounding the oocyte is essential for vitellogenesis (Lubzens et al. 2010). Therefore, using zebrafish (*Danio rerio*) as a model, the present study aimed to investigate the possibility that DNA methylation is involved in regulating *cyp19a1a* expression during ovarian folliculogenesis. This study explored the relationship between the fluctuation of the methylation levels of *cyp19a1a* core promoter and *cyp19a1a* expression levels in the progression of zebrafish ovarian folliculogenesis. As such, this methylation mechanism may contribute significantly to the initialization and maturation of ovarian folliculogenesis in diverse vertebrates.

## Materials and methods

### Animals and gonadal tissues

All zebrafish used for the present study were of the Tüebingen strain and were kept in a zebrafish facility (ESEN, China) and maintained under standard conditions (Westerfield 2000). Isolation of ovarian follicles was conducted as described previously (Kwok et al. 2005). In brief, 10–20 reproductively active adult female zebrafish (3–5 months old) were euthanized in ice water and decapitated. After that, their ovaries were pooled together and quickly dispersed in a petri dish containing 60 % Leibovitz L-15 medium. The follicles of different stages were verified and manually isolated under a stereo microscope (Zeiss, Germany). The development of ovarian follicles was classified into six stages based on the diameter, namely primary growth (diameter ≤ 100 μm, PG), pre-vitellogenic (100–300 μm, PV), early-vitellogenic (300–400 μm, EV), mid-vitellogenic (400–500 μm, MV), late-vitellogenic (500–600 μm, LV), and full-grown stage (≥650 μm, FG). For each developmental stage, at least 40 ovarian follicles were pooled as one parallel sample.

### Quantification of *cyp19a1a* expression

For gene expression analysis, total RNA was isolated from ovarian follicle sample at each developmental stage using RNAzol® RT RNA isolation reagent (MRC, Cincinnati, OH, USA). The same amount of total RNA (2 μg) was used for synthesis of the first-strand cDNAs using a RevertAid First Strand cDNA Synthesis Kit (Thermo Scientific, USA) following the manufacturer's instructions. The relative expression levels of zebrafish *cyp19a1a* and housekeeping gene *ef1α* were detected using real-time quantitative PCR (qPCR) with gene-specific primers (Table 1), which were examined for their specificity and amplification efficiency on serial dilutions of respective target gene plasmid DNA ($2 \times 10^2$–$2 \times 10^7$ copies/2 μL) (results not shown). The relative mRNA levels of the target genes were determined using the comparative $C_t$ method (Schmittgen and Livak 2008). The results from four parallel samples were quantified and averaged.

### Determination of DNA methylation level using sodium bisulfite genomic sequencing

To determine global DNA methylation level at different follicular stages, genomic DNA from zebrafish PV, EV, MV, LV, FG follicles, and live tissue were extracted with a TIANamp Marine Animals DNA Kit (Tiangen Biotech, Beijing, China) following the manufacturer's protocol except for the following modifications: Homogenized ovarian follicles were

**Table 1** Primers used in the present study

| Primer name | Sequence (5′–3′) |
|---|---|
| Quantitative real-time PCR primers for *cyp19a1a* gene expression analysis | |
| *cyp19a1a*qF | GTTCAGTCTTGACAACTTCCATAAAAAT |
| *cyp19a1a*qR | TGCGACAGGTTGTTGGTTTGC |
| *ef1α*qF | GGCTGACTGTGCTGTGCTGATTG |
| *ef1α*qR | CTTGTCGGTGGGACGGCTAGG |
| *βactinqF* | TCCCCTTGTTCACAATAACC |
| *βactinqR* | TCTGTGGCTTTGGGATTCA |
| Nested PCR for amplification of zebrafish *cyp19a1a* core promoter | |
| Outer nested PCR | |
| *cyp19a1a*F1 | ATGAAGTGTATTAAAATAAGGATAT |
| *cyp19a1a*R1 | AACAAATCCAACTAACCTAAAATATATA |
| Inner nested PCR | |
| *cyp19a1a*F2 | TGFTTGAGTTTTATGTAGTTGTTGG |
| *cyp19a1a*R2 | CATTATCCTAAACCCTTTCAATACC |
| ChIP PCR for amplification of zebrafish *cyp19a1a* core promoter | |
| *cyp19a1a*CHIP5F | GAGGCTGTGGTGGATCTTCT |
| *cyp19a1a*CHIP5R | TTGTGTGGTCGATGGTGTCT |

digested for 1 h with proteinase K (40 mg/mL) to eliminate the high content of yolk protein; DNA was treated with RNAase to remove RNA contaminants; and DNA concentrations were quantitated with Nanodrop 2000 (Thermo Scientific, Wilmington, DE, USA).

Half a microgram of genomic DNA from each developmental stage sample was treated with sodium bisulfite, using the EZ DNA Methylation$^{TM}$ Kit (USA) following the manufacturer's instructions. Nested PCR amplification was carried out using primers specific for bisulfite-converted DNA sequence targeted to a core region (−74 to +125) close to the *cyp19a1a* transcriptional starting site (TSS) (Table 1). The outer nested PCR conditions were as follows: 5 min at 94 °C; 35 cycles of 30 s at 94 °C, 30 s at 55 °C, and 30 s at 72 °C; and 5 min at 72 °C. Inner nested PCR conditions for the *cyp19a1a* core promoter were the same as the outer nested PCR conditions. The resulting PCR products were gel-purified and cloned into pMD19-T (Takara). About 12–15 colonies from each PCR product were picked up for further sequencing. The resulting sequences were examined for conversion efficiency and accuracy, using BiQ analyzer software. Sequences with less than a 98 % conversion rate were not analyzed. Based on the sequence results, for the methylation levels of the core promoter case, we firstly calculated the percentage of the number of the methylated CpG dinucleotides out of seven from one colony and further repeated this step of other colonies. For the methylation levels of the individual CpG dinucleotides site case, we firstly calculated the percentage of the number of the methylated CpG dinucleotides out of the number of the colonies of one batch from one independent experiment and further calculated the average value of other batches of samples. The results from at least three independent experiments were quantified and averaged.

### Determination of methylation level with combined bisulfite restriction analysis (COBRA)

For COBRA, half of the inner nested PCR products amplified from the bisulfite-treated genomic DNA were digested with RsaI (Fermentas) (Fig. 3a), and the other half was used as an undigested control. According to a previous study, aromatase is specifically expressed in the brain and gonad but not in the liver (Chiang et al. 2001). The PCR products amplified from the unmethylated bisulfite-treated genomic DNA remained intact following RsaI digestion, whereas those from the methylated genomic DNA were fragmented. In this way, the PCR products amplified from the bisulfite-treated genomic DNA from the liver could be totally digested, working as a control of

complete digestion. After separating on a 3.0 % agarose gel, the intensity of each band from digested and undigested PCR products was quantified using Gel-Pro 4.0 Software. The concept of methylation degree acted as a means of quantifying the methylation level. The methylation degree in each sample was calculated using the formula $(I^{Me}/(I^{U} + I^{Me})) \times 100$, where $I^{Me}$ and $I^{U}$ represent the intensities of the methylated and unmethylated bands, respectively. The results from at least three independent experiments were quantified and averaged.

### Chromatin Immunoprecipitation (ChIP) assay

ChIP assays were performed with an EZ ChIP assay kit (Millipore, CA, USA) following the manufacturer's protocol with minor modifications. In brief, 0.1 g ovarian follicles at the same developmental stage were put into 400 μL PBS buffer containing protease inhibitor cocktail II on ice and fixed in 1 % (v/v) freshly prepared formaldehyde for 15 min. After homogenizing on ice, 1 mL glycine was added to quench any unreacted formaldehyde at room temperature for 10 min. The resulting tissue suspension was centrifuged, washed twice, and resuspended in 1 mL SDS lysis buffer containing protease inhibitor cocktail II. Chromatin was sonicated into 0.2–0.8 kb lengths using a sonicator with a microtip. The sheared chromatins obtained from the ovarian follicles were immunoprecipitated following the manufacturer's protocol with 2 μg of specific antibody against RNA polymerase II or with 1 μg of normal mouse IgG (as negative control) at 4 °C overnight. Immunoprecipitated chromatin was then used as the template for PCR amplification of the *cyp19a1a* core promoter (+61/+201) using primers *cyp19a1a*ChIP5F and *cyp19a1a*-ChIP5R as listed in Table 1. The product was separated on 3 % agarose gels and visualized using staining with ethidium bromide.

### Statistical analysis

Differences among groups were analyzed with one-way ANOVA followed by the Tukey's post hoc test (for comparing all pairs of groups). The analyses were performed using the GraphPad Prism 5 software package (San Diego, CA, USA).

## Results

### Temporal expression profile of *Cyp19a1a* transcripts during folliculogenesis

Because of the asynchronous folliculogenesis in zebrafish, we could obtain and identify ovarian follicles at different stages based on their diameters. Our results demonstrate that *cyp19a1a* transcript expression levels exhibit a clear stage-dependent pattern. At the PV stage, *cyp19a1a* transcripts exhibit the lowest expression level. The expression levels increase significantly at the MV stage and reach a peak at the LV stage. However, after the follicles develop into the FG stage, *cyp19a1a* transcript expression level drops significantly (Fig. 1).

### Dynamic methylation levels of the core promoter of *cyp19a1a* during folliculogenesis

The core promoter of the zebrafish *cyp19a1a* gene includes a TATA box (−47), a transcriptional starting site (TSS), and seven CpG dinucleotide sites (from −35 to +100) (Fig. 2a). The methylation level of the core promoter of zebrafish *cyp19a1a* gene is determined using sodium bisulfite sequencing. At the MV

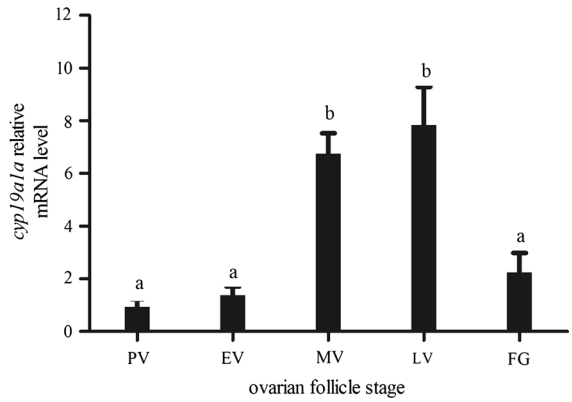


**Fig. 1** Stage-dependent relative expression levels of *Cyp19a1a* mRNA during ovarian folliculogenesis in sexually mature gravid zebrafish. The levels of the respective mRNAs were determined using qPCR and normalized to the housekeeping gene (*ef1α*). Data are expressed as the mean ± SEM ($n = 4$) relative to the respective transcript levels measured in the PV stage. *Bars* marked with *different letters* are significantly different from each other ($p < 0.05$, one-way ANOVA followed by the Tukey's post hoc test). *PV* pre-vitellogenic, *EV* early-vitellogenic, *MV* mid-vitellogenic, *LV* late-vitellogenic, and *FG* full-grown stage

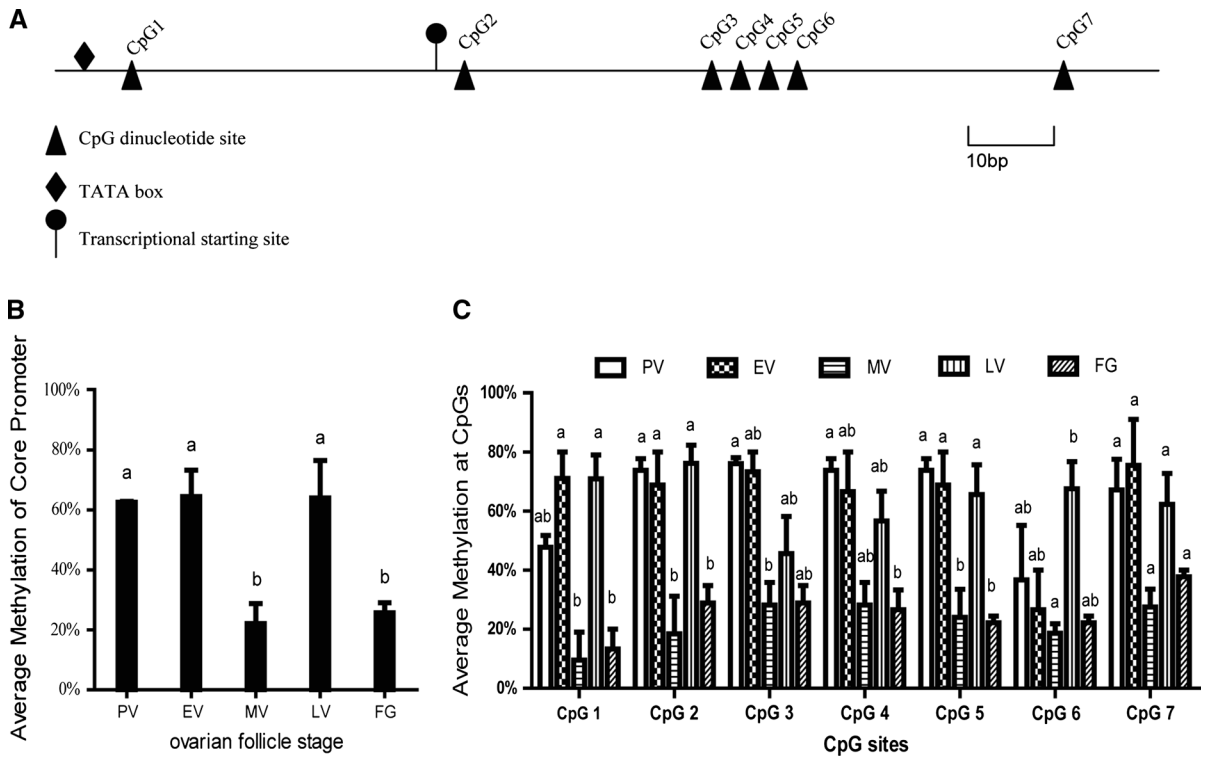


**Fig. 2** Dynamic methylation levels of the *cyp19a1a* gene core promoter during ovarian folliculogenesis in zebrafish. **a** Schematic diagram of CpG dinucleotide sites 1–7 (indicated by *filled circles*) distribution and putative sites for TATA box in core promoter of zebrafish *cyp19a1a.* **b** The percentage of methylated cytosine of all CpG dinucleotides within the core promoter. Methylation level was determined by sequencing bisulfite-treated genomic DNA extracted from ovarian follicles. *Bars* marked with *different letters* were significantly different from each other. *Each bar* represents the mean ± SEM ($n = 3$). ($p < 0.05$, one-way ANOVA followed by the Tukey's post hoc test). **c** The percentage of methylated cytosine of individual CpG dinucleotide site within the core promoter. Methylation level was determined by sequencing bisulfite-treated genomic DNA during ovarian fulliculogenesis. *Bars* marked with *different letters* were significantly different from each other. *Each bar* represents the mean ± SEM ($n = 3$). ($p < 0.05$, one-way ANOVA followed by the Tukey's post hoc test). *PV* pre-vitellogenic, *EV* early-vitellogenic, *MV* mid-vitellogenic, *LV* late-vitellogenic; and *FG* full-grown stage

and FG stages, the average methylation levels are lowest, whereas at PV, EV and LV stages methylation levels are much higher (Fig. 2b). Except the seventh CpG dinucleotide site, all the rest CpG dinucleotide sites show a significant fluctuation pattern that appears to be lower at MV and FG stages than at EV, PV, and LV stages (Fig. 2c).

Results from COBRA indicated that all genomic DNA from different ovarian follicular stages are digested by RsaI at different levels (Fig. 3b, c). Methylation degrees at MV and FG stages show two significantly low levels which are consistent with the pattern of total average methylation level fluctuation (Figs. 2b, c, 3c). In the control, only fragmented genomic DNA could be observed from the liver, which suggests a totally methylated level (Fig. 3b).

### Binding status of RNA polymerase II to the core promoter of *cyp19a1a* during folliculogenesis

ChIP assays are carried out to further examine the binding of RNA polymerase II to zebrafish *cyp19a1a* core promoter. The RNA polymerase II is recruited to *cyp19a1a* core promoter stronger at the MV stage rather than at the EV, LV and FG stages (Fig. 4). Also, at the EV and FG stages, RNA polymerase II binding is barely detectable.

## Discussion

In the present study, for the first time, the results from both sodium bisulfite genomic sequencing and

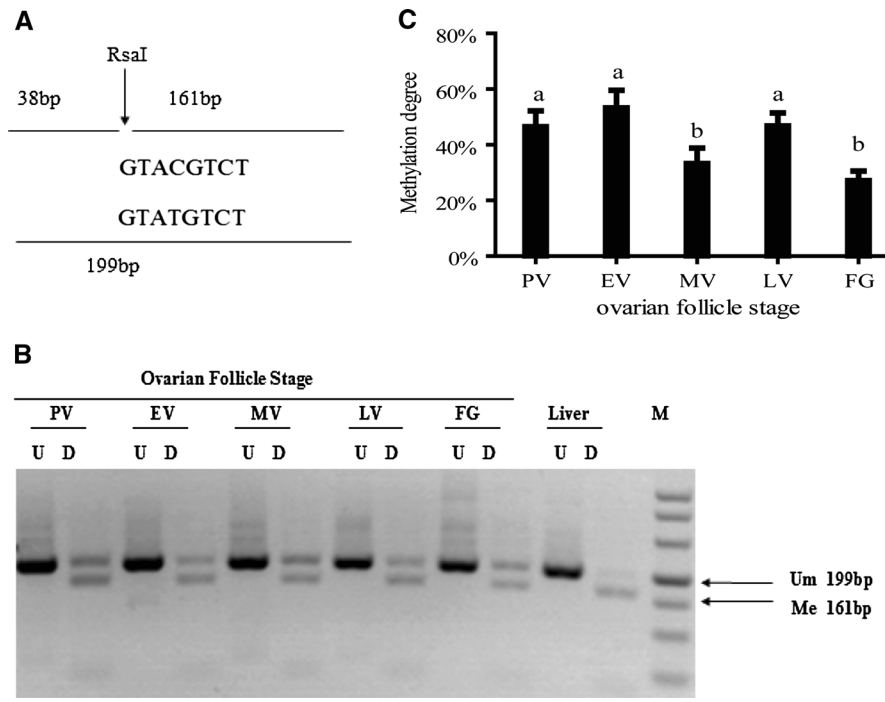


**Fig. 3** DNA methylation levels of *cyp19a1a* core promoter during zebrafish ovarian folliculogenesis. **a** Schematic diagram showing the strategy of combined bisulfite restriction analysis (COBRA). **b** The representative electrophotogram showing methylation levels analyzed using COBRA. The liver genomic DNA was used as control. *U*, undigested; *D*, digested with RsaI restriction enzyme; *M*, *DL* 500 marker. PCR products from the unmethylated DNA were intact (Um), whereas the PCR products from the methylated DNA were fragmented (Me). The experiments were repeated at least three times. **c** Methylation degree. The methylation degree was calculated based on the band intensities from methylated and unmethylated templates. *Each bar* represents the mean ± SEM ($n = 3$). *Bars* marked with *different letters* are significantly different from each other ($p < 0.05$, one-way ANOVA followed by the Tukey's post hoc test). *PV* pre-vitellogenic, *EV* early-vitellogenic, *MV* mid-vitellogenic, *LV* late-vitellogenic, and *FG* full-grown stage

COBRA clearly show that during ovarian folliculogenesis there is an apparent fluctuation of the methylation levels of zebrafish *cyp19a1a* core promoter, which suggests that epigenetic mechanisms may participate in the regulation of *cyp19a1a* expression during ovarian folliculogenesis in adult female zebrafish.

Several reports show that the gonadotropin stimulation of $E_2$ production in teleost vitellogenic ovarian follicles is accompanied by increased expression of *cyp19a1a* (Kagawa et al. 2003; Montserrat et al. 2004). In the present study, we observe that the expression levels of *cyp19a1a* transcripts show a significant increase when the ovarian follicles develop into the MV stage, which are consistent with previous results of in situ hybridization (Chiang et al. 2001). Interestingly, this expression pattern is inversely correlated with the average methylation levels during zebrafish early ovarian folliculogenesis (from the PV to the MV stage). As in mammals (Stocco 2008), studies in trout and ricefield eel demonstrate that the stimulation of *cyp19a1a* by gonadotropins in the ovary is mainly mediated by cAMP (Planas et al. 1997; Zhang et al. 2013), which can be explained by the cAMP response element (CRE), a conserved feature in *cyp19a1a* promoters of several teleost species (Zhang et al. 2013). Although there is no CRE within the core promoter region examined in the present study, the results from ChIP assay indicate that the binding of RNA polymerase II to zebrafish *cyp19a1a* core promoter dramatically increases when the ovarian follicles develop into the MV stage, which is confirmed by the sodium bisulfite genomic sequencing results showing that the average methylation levels of the first and second CpG dinucleotide sites which are closed to the TATA box and TSS exhibit the lowest methylation levels at the MV stage. Although we could not exclude the possibility that the increase of

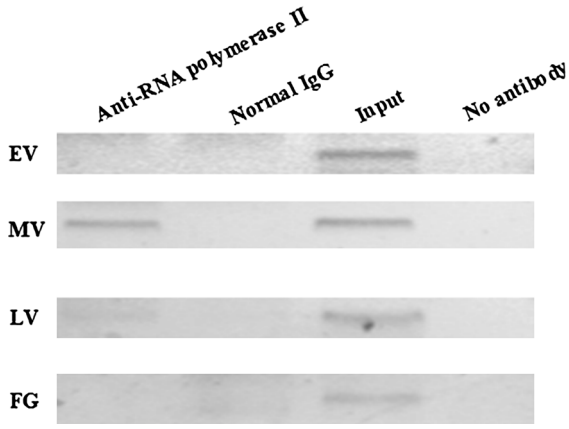


**Fig. 4** Binding status of RNA polymerase II to *cyp19a1a* promoter in zebrafish ovarian follicles at different developmental stages. A ChIP was performed as described in the "Materials and methods". The DNA fragments were immunoprecipitated using antibodies against RNA polymerase II and normal mouse IgG; PCR amplified using primer sets corresponding to zebrafish *cyp19a1a* core promoter; separated on 3.0 % agarose gels; and visualized by staining with ethidium bromide. *EV* early-vitellogenic, *MV* mid-vitellogenic, *LV* late-vitellogenic, *FG* full-grown stage

*cyp19a1a* transcript levels is mediated by gonadotropins, one recent study demonstrates that once entering the PV stage, the ovarian follicles in follicle-stimulating hormone β knocked out zebrafish could quickly restore the growth to complete the process of vitellogenesis (Zhang et al. 2014). Taken together, this information suggests that the increase of *cyp19a1a* expression levels during early folliculogenesis is depended on both the mechanisms of the epigenetic modifications of the *cyp19a1a* core promoter and gonadotropin regulation.

In teleosts, the major endocrine events associated with the termination of the vitellogenesis and the progression to meiosis resumption (oocyte maturation) are an acute increase in plasma LH levels, which causes a switch in the steroidogenic pathway in ovarian follicles from the synthesis of estrogens to the production of the progestins 17,20β-dihydroxy-4-pregnen-3-one and 17,20β,21-trihydroxy-4-pregnen-3-one, by altering the expression of steroidogenic enzymes involved in their synthesis (Lubzens et al. 2010). Results from the present study clearly showed a down-regulation of *cyp19a1a* transcript levels, when zebrafish ovarian follicles developed from the LV to the FG stage. The similar expression pattern, i.e., a dramatic decrease in aromatase expression during final oocyte maturation, is also reported in several teleost species, e.g., channel catfish (*Ictalurus punctatus*) (Sampath Kumar et al. 2000), rainbow trout (*Oncorhynchus mykiss*) (Nakamura et al. 2005), and Atlantic croaker (*Micropogonias undulatus*) (Nunez and Applebaum 2006). However, the molecular mechanism that mediates this decrease in *cyp19a1a* gene expression during is still unknown. In the present study, the increasing methylation levels of *cyp19a1a* core promoter at the LV stage may suggest that the ovarian follicles might start to terminate the production of *cyp19a1a* transcripts, which is further confirmed by the results of ChIP assay that the binding of RNA polymerase II to zebrafish *cyp19a1a* core promoter dramatically decreases when ovarian follicles develop into the LV stage. Apparently, the methylation of *cyp19a1a* core promoter cannot immediately result in the decrease in expression levels of *cyp19a1a* transcripts. This may explain our results that *cyp19a1a* transcripts level at the LV stage is similar to that at the MV stage, which is most likely due to the delay in the degradation of *cyp19a1a* transcripts mainly produced at the MV stage.

When ovarian follicles develop into the FG stage, although the methylation levels of *cyp19a1a* core promoter decrease significantly, the binding of RNA polymerase II to zebrafish *cyp19a1a* core promoter is as weak as that of LV stage, which may partially result in the dramatic decrease in *cyp19a1a* transcripts at the FG stage. In the meantime, the regulation mechanism at the posttranscriptional level may also be involved in this dramatic decrease in *cyp19a1a* transcripts at the FG stage. Study in a porcine model has demonstrated that the aromatase expression, and therefore the estradiol production, by granulosa cells, is posttranscriptionally down-regulated by Micro-RNA378 (Xu et al. 2011), which also alters the gene expression and function in cumulus cells and influences oocyte maturation, possibly via oocyte–cumulus interaction and paracrine regulation (Pan et al. 2015). This claim remains rather speculative as further experimental evidence is yet to be obtained.

In summary, we have demonstrated, for the first time in a teleost species, that the methylation levels within the *cyp19a1a* core promoter may participate in the regulation of *cyp19a1a* during zebrafish ovarian folliculogenesis. This dynamic DNA methylation fluctuation may coexist with gonadotropin in regulating *cyp19a1a* expression during ovarian folliculogenesis.

Further studies are necessary to illuminate the mechanisms of stage-dependent epigenetic control during ovarian folliculogenesis.

**Acknowledgments** This work was supported in part by the Marine Science Base Project for Scientific Research Training and Capacity Enhancement—Xiamen University, the National Natural Science Foundation of China (Nos. J1210050 and 31201977), the Natural Science Foundation of Fujian Province (No. 2013J05029), and Xiamen Southern Oceanographic Center (No. 14GZY019NF19). Professor John Hodgkiss of The University of Hong Kong is thanked for his help with the English.

**Compliance with ethical standards**

**Conflict of interest** The authors declare that they have no conflict of interest.

## References

Chiang E, Yan Y, Guiguen Y (2001) Two *Cyp19* (P450 aromatase) genes on duplicated zebrafish chromosomes are expressed in ovary or brain. Mol Biol Evol 18:542–550

Duffy T, Picha M, Won E, Borski R, McElroy A, Conover D (2010) Ontogenesis of gonadal aromatase gene expression in Atlantic silverside (*Menidia menidia*) populations with genetic and temperature-dependent sex determination. J Exp Zool 313A:421–431

Fürbass R, Selimyan R, Vanselow J (2008) DNA methylation and chromatin accessibility of the proximal *Cyp19* promoter region 1.5/2 correlate with expression levels in sheep placentomes. Mol Reprod Dev 75:1–7

Guengerich FP (2007) Cytochrome p450 and chemical toxicology. Chem Res Toxicol 21:70–83

Kagawa H, Gen K, Okuzawa K (2003) Effects of luteinizing hormone and follicle-stimulating hormone and insulin-like growth factor-I on aromatase activity and P450 aromatase gene expression in the ovarian follicles of red seabream, Pagrus major. Biol Reprod 68:1562–1568

Knower KC, To SQ, Simpson ER (2010) Epigenetic mechanisms regulating CYP19 transcription in human breast adipose fibroblasts. Mol Cell Endocrinol 321:123–130

Kwok H-F, So W-K, Wang Y, Ge W (2005) Zebrafish gonadotropins and their receptors: I. Cloning and characterization of zebrafish follicle-stimulating hormone and luteinizing hormone receptors—evidence for their distinct functions in follicle development. Biol Reprod 72:1370–1381

Lee L, Asada H, Kizuka F (2012) Changes in histone modification and DNA methylation of the StAR and Cyp19a1 promoter regions in granulosa cells undergoing luteinization during ovulation in rats. Endocrinology 154:458–470

Lubzens E, Young G, Bobe J, Cerdà J (2010) Oogenesis in teleosts: how fish eggs are formed. Gen Comp Endocrinol 165:367–389

Monga R, Ghai S, Datta TK (2011) Tissue-specific promoter methylation and histone modification regulate *CYP19* gene expression during folliculogenesis and luteinization in buffalo ovary. Gen Comp Endocrinol 173:205–215

Montserrat N, González A, Méndez E, Piferrer F, Planas JV (2004) Effects of follicle stimulating hormone on estradiol-17β production and P-450 aromatase (CYP19) activity and mRNA expression in brown trout vitellogenic ovarian follicles in vitro. Gen Comp Endocrinol 137:123–131

Nakamura I, Evans JC, Kusakabe M, Nagahama Y, Young G (2005) Changes in steroidogenic enzyme and steroidogenic acute regulatory protein messenger RNAs in ovarian follicles during ovarian development of rainbow trout (Oncorhynchus mykiss). Gen Comp Endocrinol 144:224–231. doi:10.1016/j.ygcen.2005.06.004

Navarro-Martín L, Viñas J, Ribas L, Díaz N, Gutiérrez A, Di Croce L, Piferrer F (2011) DNA methylation of the gonadal aromatase (*cyp19a*) promoter is involved in temperature-dependent sex ratio shifts in the European sea bass. PLoS Genet 7:e1002447

Nunez BS, Applebaum SL (2006) Tissue- and sex-specific regulation of CYP19A1 expression in the Atlantic croaker (Micropogonias undulatus). Gen Comp Endocrinol 149:205–216. doi:10.1016/j.ygcen.2006.06.005

Pan B, Toms D, Shen W, Li J (2015) MicroRNA-378 regulates oocyte maturation via the suppression of aromatase in porcine cumulus cells. Am J Physiol Endocrinol Metab 308:E525–E534. doi:10.1152/ajpendo.00480.2014

Piferrer F, Blázquez M (2005) Aromatase distribution and regulation in fish. Fish Physiol Biochem 31:215–226

Planas JV, Goetz FW, Swanson P (1997) Stimulation of brook trout ovarian steroidogenesis by gonadotropins I and II is mediated by the cyclic adenosine 3′, 5′-monophosphate/protein kinase A pathway. Biol Reprod 57:647–654

Sampath Kumar R, Ijiri S, Trant JM (2000) Changes in the expression of genes encoding steroidogenic enzymes in the channel catfish (*Ictalurus punctatus*) ovary throughout a reproductive cycle. Biol Reprod 63:1676–1682

Schmittgen T, Livak K (2008) Analyzing real-time PCR data by the comparative $C_T$ method. Nat Protoc 3:1101–1108

Stocco C (2008) Aromatase expression in the ovary: hormonal and molecular regulation. Steroids 73:473–487

Tchoudakova A, Callard GV (1998) Identification of multiple CYP19 genes encoding different cytochrome P450 aromatase isozymes in brain and ovary. Endocrinology 139:2179–2189

Westerfield M (2000) The zebrafish book: a guide for the laboratory use of zebrafish (*Danio rerio*). University of Oregon Press, Eugene

Xu S, Linher-Melville K, Yang BB, Wu D, Li J (2011) MicroRNA378 (miR-378) regulates ovarian estradiol production by targeting aromatase. Endocrinology 152:3941–3951. doi:10.1210/en.2011-1147

Zhang Y, Zhang S, Liu Z, Zhang L, Zhang W (2013) Epigenetic modifications during sex change repress gonadotropin stimulation of Cyp19a1a in a teleost ricefield eel (*Monopterus albus*). Endocrinology 154:2881–2890

Zhang Z, Zhu B, Ge W (2014) Genetic analysis of zebrafish gonadotropin (FSH and LH) functions by TALEN-mediated gene disruption. Mol Endocriol 29:76–98